

A verdant approach to the synthesis of silver nanoparticles using the leaf extracts of Jackfruits; estimation of the antioxidant and photocatalytic activity, antibacterial properties, melamine adulteration in milk, Para nitrophenol catalysis and cytotoxicity studies.

Thisha Ranjan¹, Mathivathani Kandiah^{1*}, Ominda Perera¹ and Beneli Gunartne¹

¹Faculty of Life and Medical Sciences, Business Management School (BMS), Sri Lanka

*mathi@bms.ac.lk

Abstract

Nanotechnology is a vast area which attracts researchers due to molecules being within the nanoscale. *Artocarpus heterophyllus* is a medicinal fruit with many health benefits. In this study, five different variants of Jackfruit leaves; Red, Durian, Maharagama, Mandoor and Nirosha were used to synthesize silver nanoparticles (AgNP) via green approach. The shape and size of the AgNP was analyzed using a scanning electron microscope, which showed spherical AgNP in the range of 20-60 nm. The water extracts (WE) and their AgNP were evaluated on their total flavonoid content, total phenolic content and total antioxidant content, which showed higher values for AgNP. The antioxidant activity was determined via the 2,2-diphenyl-1 picrylhydrazyl assay and their IC₅₀ value was determined, showing that the Durian and Mandoor WE had an IC₅₀ higher than their AgNP. The cytotoxicity of AgNP was determined using *Artemia salina* and all of them had a 100% viability. The degradation of para-nitrophenol was also observed in the presence of AgNP and Durian_AgNP showed the highest degradation rate. Furthermore, the photocatalytic degradation of methylene blue was performed with 4000 ppm and 266.67 ppm AgNP. 4000 ppm AgNP showed a faster degradation in the presence of NaBH₄ and no visible degradation was observed under sunlight. Detection of melamine in milk was performed using Mandoor_AgNP, melamine was detected in water but not in milk. Lastly, the antibacterial activity was tested against *E. coli* and *S. aureus* using the well diffusion method. A zone of inhibition was observed with all the AgNP with *E. coli* and *S. aureus*. These research findings can be utilized in drug delivery, as alternatives for antibiotics and in the degradation of dye before entering the environment.

Keywords: *Artocarpus heterophyllus*, Green Synthesis, Scanning Electron Microscope (SEM), Silver Nanoparticles (AgNP), Melamine, Antioxidants

1. Introduction

Nanotechnology is a vast area that attracts many researchers due to its contribution in fields like science, engineering and computer science. "Nanoscience is the study of structures and molecules on the scales of nanometers ranging between 1 and 100 nm, and the technology that utilizes it in practical applications is called nanotechnology."¹⁰

Nanoparticles are materials that have a dimension within the nanoscale.⁴⁵ There are many types of nanoparticles out of which AgNP have drawn great attention in recent years due to its chemical stability, increased surface area to volume ratio, anti-microbial properties, catalytic activity,⁷¹ along with optical, thermal and electrical conductivity.⁷⁹ AgNP has a

variety of applications in anti-cancer therapy, wound healing and drug delivery.¹⁵ It is also used in cosmetics, textile, electronics, sensors and water treatments.³²

Metal nanoparticles can be synthesized using 2 approaches; the top-down approach and the bottom-up approach, illustrated in Figure 01. In the top-down approach, bulk materials are used as the starting material for nanoparticle synthesis. Bottom-up approach starts with atoms and builds on to produce nanoparticles.⁷⁶ Under these two approaches, there are three ways to synthesize nanoparticles, which are physical, chemical and biological methods.

Physical method uses techniques like laser ablation and evaporation-condensation.³⁶ This uses mechanical processes to reduce the size of the bulk material.⁷⁶ In chemical methods, the silver precursors are reduced by organic/inorganic solvents which leads to AgNP synthesis.⁴⁶ Biological methods or the green approach involves the use of plants and microbes, causing it to be an eco-friendly, cost-effective, simple approach yet high yield of AgNP can be produced.⁷⁷ In this research plants were used as the use of microbes requires time and aseptic conditions.²

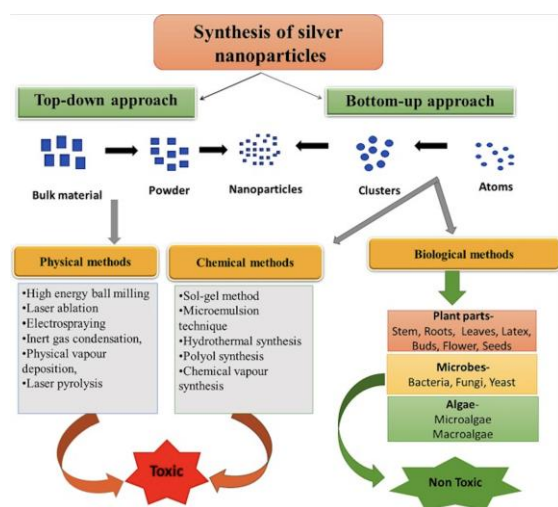


Figure 01: Different methods of AgNP synthesis.²⁰

Artocarpus heterophyllus or Jackfruits are known for its taste, appearance as well as its health benefits. However, the pulp and seeds of the fruit is usually consumed and the other parts like the rind and leaves are often wasted despite them having many health benefits such as high antioxidant activity, the ability to control blood glucose levels, possessing anticarcinogenic, antimicrobial, anti-inflammatory and for wound healing.⁵⁵ Therefore, this research focuses on the synthesis of AgNP using Jackfruit leaves and performing various other tests from the synthesized AgNP and evaluating their results. In this research, five different variants of Jackfruit leaves were used: Red, Durian, Maharagama (MG), Mandoor and Nirosha.

Substances (natural or synthetic) that prevent or delay cellular damage caused by oxidants are known as antioxidants.¹¹ These oxidative stresses are associated with diseases like cancer, diabetes, atherosclerosis, Alzheimer's

disease.²⁵ The AgNP can act as an antioxidant either by the single electron transfer or the hydrogen transfer and thus prevents or delay the damages caused to the cell by the oxidative stresses.¹²

Since nanoparticles can be used in the health field, it is important to test for its possible toxicity before its final use in the industry. *Artemia salina* (brine shrimps) are used to test for the lethality of AgNP. These are common model organisms, as it is cost-effective, has a short life cycle, increased offspring production and easy availability of the cysts.⁸ The nauplii has a higher sensitivity to the toxic components compared to the adult brine shrimp. Other techniques to detect toxicity in cells include dye exclusion, colorimetric and fluorometric assays. However, these have their disadvantages such as insensitivity, time-consuming and labor intensive.⁷

Para-nitrophenol (PNP) is a toxic substance released from the dye, explosives and pesticides industries that causes harm to the environment, especially to the aquatic system and humans.⁶³ Since PNP degradation is too slow, the AgNP acts as a catalyst and allows the reaction to proceed. Advantages of AgNP involve them being biodegradable, cost-effective and the lack of secondary pollution production.⁶³ Despite there being other techniques like electro or photocatalyst and adsorption, these use high energy and expensive instruments.⁷⁵

Synthetic dyes are widely used in the textile industries, where the waste is discarded into the water system. These dyes are either non-biodegradable³⁵ or can be transformed into carcinogens upon degradation of microbes present inside humans or animals. Even though, there are many wastewater treatment processes like reverse osmosis, incineration, filtration, electrochemical oxidation, they have their disadvantages such as the production of volatile toxic gases, increased reaction time, smelly odour, sludge formation and more.⁶⁰ Since AgNP have a large surface area, high adsorption properties and increased equilibrium rates, they can be used in the removal of these harmful dyes before entering the water system.⁴²

Melamine is a chemical compound rich in nitrogen that is used as an adulterant in dairy

products, to increase their protein content. AgNP can be used in the detection of melamine (in milk) using colorimetric methods.³⁴ Melamine can also be detected by gas chromatography and high-performance liquid chromatography. In contrast, these techniques are time consuming, involve the use of expensive equipment, extensive sample preparation and require skilled personnel.⁵⁷

Recently, antibiotics were becoming less effective against bacteria due to the increased usage and mutations in the bacterial cell. It is difficult to develop new antibiotics, as it is time consuming to study the efficacy and safety of the new drug and a large number of resources are needed. Meanwhile, the infections from the resistant microbes continue to spread.¹⁴ Therefore, AgNP can be an excellent alternative to antibiotics, due to their antibacterial properties of releasing Ag^+ ions, inducing oxidative stress and the surface-binding of the bacteria to the AgNP, making it difficult for the bacteria to develop resistance against AgNP,⁶⁵ thus, allowing AgNP to be incorporated into medical products like catheters and other surgical tools.

This study aimed to investigate the use of leaf extracts from five different variants of Jackfruits to synthesize AgNP. The AgNP produced was used in assessing their antioxidant and photocatalytic activity, antibacterial properties, melamine adulteration in milk, para-nitrophenol catalysis and cytotoxicity studies. Scanning electron microscope (SEM) was used to analyze the shape and size of the AgNP. 2,2-diphenyl-1-picrylhydrazyl (DPPH) assay was used in the estimation of the antioxidant properties, whereas methylene blue (MB) and NaBH_4 was used in the estimation of the photocatalytic activity. As for the PNP catalysis, the synthesized AgNP was used to catalyze the reaction between PNP and NaBH_4 . *E. coli* and *S. aureus* were used in the evaluation of the antibacterial properties via well diffusion and the cytotoxicity was tested on *Artemia salina*. Hence, utilizing this research results in wastewater treatment, industrial and medical fields.

2. Methodology

Throughout the research, a good laboratory practice was followed along with the use of personal protective equipment.

2.1 Sample Collection. In this research, five different variants of Jackfruit leaves, collected from Diyatha Uyana, Battaramulla were used. The variants used are Red, Durian, Maharagama (MG), Mandoor and Nirosha, illustrated in Figure 02.

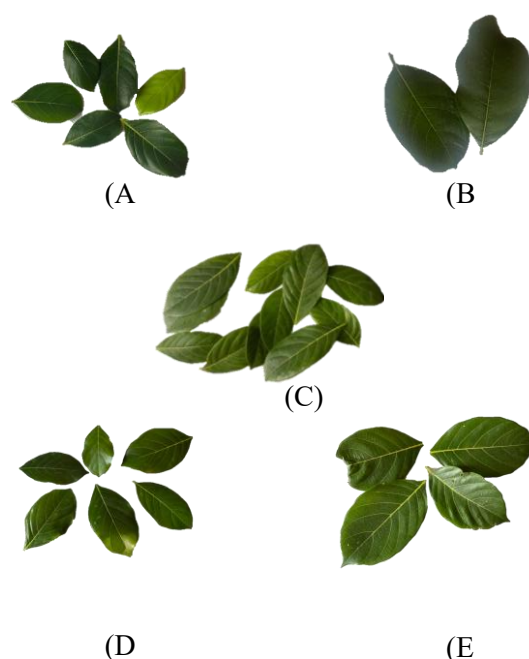


Figure 02: Different variants of Jackfruit leaves; (A) Red (B) Durian (C) MG (D) Mandoor (E) Nirosha

2.2 Preparation of water extraction of Jackfruit leaves. Dried Jackfruit leaves were cut into smaller pieces and 2 g of each variant was soaked in 50 mL distilled water ($\text{d.H}_2\text{O}$). This was placed in the hot oven for 1 hour at 100°C and was then allowed to cool. Afterwards, all the five different water extracts (WE) were filtered using Whatman Filter paper and were stored at -4°C until further use.³⁹

2.3 Qualitative analysis of phytochemicals. This qualitative analysis was performed with WE.

Table 01: Shows the Phytochemicals test performed and their expected results.

Phytochemical Tests	Methodology	Expected Results
Alkaloids	A volume of 0.5 mL from each WE were placed into an oven to obtain residues. Afterwards, 1.5mL of the 2% (v/v) HCl was added into the WE residues and was dissolved. To this 1 drop of Mayer's reagent was added.	A white precipitate. ⁶⁶
Amino acids	Ninhydrin reagent (2 drops) was added into 0.5 mL of WE and was heated in a water bath	Colour change to blue. ¹³
Anthocyanins	A volume of 0.5 mL of concentrated HCl was added into 0.5 mL of WE	Anthocyanins appear red in acidic conditions. ³¹
Carbohydrates	To 0.5 mL WE, 2 drops of Iodine solution was added	Blue-black colour observed. ²³
Flavonoids	A volume of 125 μ L of 1% AlCl_3 was added into 0.5 mL of WE.	Colour changes to yellow. ⁴⁰
Glycosides	WE (0.5 mL) were placed in an oven to reduce their volume in half. To this 0.5 mL of NH_4OH was added and was shaken.	Cherish red colour. ⁶⁶
Phenols	A total of 2 drops of 10% ferric chloride was added into 0.5mL of WE	Colour changes to black. ⁴⁰
Reducing sugars	To 0.5 mL of each WE, 1mL of Benedict's reagent was added and was heated in a water bath	Brick red indicates a positive result for reducing sugar. ¹³
Saponin	A volume of 0.5 mL of the WE were added in their respective test tubes and were shaken vigorously using a Vortex meter.	Observation of foams on the surface of the test tube. ⁶⁶
Tannin	A total of 3 drops of 1% ferric chloride was added into 0.5 mL of WE	Colour changes to black. ¹³

2.4 Synthesis of AgNP. A volume of 1 mL of the prepared WE was mixed with 9 mL of 0.02M AgNO_3 .⁴¹ This was then placed in the hot air oven at 90 °C and 60 °C for 15, 30, 45 and 60 minutes as well as at room temperature for 24 hours. A spectrophotometer reading was recorded in the range 320-520 nm with distilled water as the blank.

2.5 Evaluation of the Bandgap energy of AgNP. Bandgap energy is the energy required for an electron to move from the valence band (VB) to the conduction band (CB).²⁴

Equation 01:

$$E = h \times \frac{c}{\lambda}$$

E = Bandgap energy

h = Plank's constant (6.626×10^{-34} Js)

c = Speed of light (3×10^8 ms⁻¹)

λ = Wavelength of AgNP

2.6 SEM Analysis. An aliquot of Red_AgNP was centrifuged at 13,000 rpm for 30 seconds and the supernatant was removed, the sample was centrifuged each time after adding an aliquot of Red_AgNP and the supernatant was removed until a prominent pellet was obtained. Afterwards, this was allowed to dry in a hot air oven at 40°C and was sent to Sri Lanka Institute of Nanotechnology (SLINTEC).

2.7 Quantitative analysis of TFC, TPC and TAC of WE and AgNP. The WE and AgNP were diluted before these studies were performed. All these studies were done in triplicates and d.H₂O was used as the blank.

2.7.1 Total Flavonoid Content (TFC)

A volume of 1 mL of 20% AlCl_3 was added into 1 mL of the samples and a drop of acetic acid was added. The absorbance was measured at 415 nm.⁴⁷ Then TFC was calculated using the quercetin as the standard curve and was expressed as $\mu\text{g}/\text{QE}/100$ g.

2.7.2 Total Phenolic Content (TPC)

A volume of 0.25 mL of 10% Folin-ciocalteu phenol reagent (FCR) was added into 0.25 mL of the sample and was mixed well. After 5 minutes, 2.5 mL of 7% Na_2CO_3 was added and was then incubated at room temperature for 90 minutes. The absorbance was then recorded at 765 nm.⁴⁷ Afterwards, TPC was calculated using the standard curve (gallic acid) and was expressed as g/GEA/100 g.

2.7.3 Total Antioxidant Capacity (TAC)

A volume of 5 mL of reagent solution was added into 0.5 mL of the sample. The reagent solution was prepared by mixing 0.60 molL⁻¹ H₂SO₄, 28 mmolL⁻¹ NaH₂PO₄ and 4 mmolL⁻¹ (NH₄)₂MoO₄ in a 1:1:1 ratio. The samples were then incubated at 95 °C for 90 minutes. Afterwards, the samples were allowed to reach room temperature before the absorbance was measured at 695 nm.⁷² TAC was then calculated using ascorbic acid as the standard curve and was expressed as g/AA/100 g.

2.8 Antioxidant Scavenging Activity of WE and AgNP via DPPH assay. DPPH solution (0.1 mM) was used as the control and methanol was used as the blank. Afterwards, 20, 40, 60, 80 and 100% of the diluted WE/AgNP were prepared and to this 1 mL of the DPPH solution was added. The absorbance was then recorded at 517 nm.⁴⁴

Equation 02:

$$\% \text{ Scavenging Activity} = \frac{\text{Absorbance(DPPH)} - \text{Absorbance(Sample)}}{\text{Absorbance(DPPH)} \times 100} \times 100$$

Then, the IC₅₀ values were calculated using the % scavenging activity (Equation 02).

2.9 Cytotoxicity studies of AgNP on Brine shrimps. Brine shrimps were hatched in filtered sea water and were placed under a light source for 24 hours. In a 96 well plate, 800 ppm and 240 ppm of AgNP were added into separate wells and were filled to a total of 250µl using seawater. This was done in triplicates. A control was also prepared using only (250µl of) seawater. To this, 2 nauplii brine shrimps were added and were incubated for 24 hours next to a light source and the % viability was calculated⁶¹ using Equation 03.

Equation 03:

$$\% \text{ Viability} = \frac{\text{TotalNo.ofviableshrimps} - \text{TotalNo.ofnonviableshrimps} \times 100}{\text{Total No.of shrimps}}$$

2.10 Degradation PNP using AgNP as a catalyst. Initially, 10⁻⁴ M of PNP and 10⁻¹ M of NaBH₄ was prepared. The absorbance of PNP from 280-520 nm was used as the control. Then the readings were taken for a mixture of 2 mL of PNP and 1 mL of NaBH₄. Lastly, 20 µL of

4000 ppm AgNP was added into 2 mL of PNP and 1 mL of NaBH₄ and the absorbances were recorded until the complete degradation of PNP was observed.²⁹ d.H₂O was used as the blank and this procedure was repeated with all the AgNP. The rate constants were then calculated using equation 04.

Equation 04:

$$\ln \ln \left(\frac{C_t}{C_0} \right) = -Kt$$

$$y = mx + c$$

$$mx = -kt$$

$$y = -kt + c$$

C_t = [PNP] at each interval

C₀ = Initial [PNP]

t = Time interval

k = Rate constant

2.11 Photocatalytic degradation of Methylene blue (MB) using AgNP. To 100 mL of 0.03 mM of MB, 1 mL of each 4000 ppm and 266.67 ppm of AgNP was added and the absorbance was recorded from 400-720 nm. This was done for 2 hours with a 30-minute interval. This was then repeated with the addition of 1 mL of NaBH₄.³³ A control was also recorded using only MB and d.H₂O was used as the blank.

2.12 Melamine Detection in AgNP. Concentrations of 2 ppm and 8 ppm melamine were spiked by adding 600 µL of melamine to 800 µL of 4000 ppm Mandoor_AgNP. The absorbance was measured from 320-720 nm and d.H₂O was used as the blank.

2.12.1 Melamine Adulteration in milk. Melamine spiked in milk involved the heating of 100mL of fresh milk, till it reached 90°C and was allowed to cool down to 60°C. To this, 25 drops of 0.25M of citric acid were added and kept at room temperature for 30 minutes.. Then it was centrifuged for 20 minutes at 4000 rpm. Afterwards, the supernatant was filtered twice using a Whatman filter paper. Then the absorbance of 600µl of milk, 600µl of melamine and 800µl of Mandoor_AgNP was measured from 320-720nm along with the absorbance of 600µl of milk and 800µl of AgNP.⁵⁴

2.13 Antibacterial Activity. Initially, 15.2 g of Mueller-Hinton agar was dissolved in 400 mL of d.H₂O and was heated on a Bunsen burner

until the agar was fully dissolved and the media turned clear. This was then autoclaved at 121 °C for 15 minutes and was poured into labelled petri dishes and was allowed to solidify. The petri dish was divided into 4 and was labelled as Positive (+), Negative (-), Sample 1 (S₁) and Sample 2 (S₂) (Figure 03). The *E. coli* and *S. aureus* inoculum was prepared by using sterile cotton swabs to collect each species and this was then suspended in individual test tubes containing saline. Afterwards, the plates were inoculated with their respective inocula. Following this, two drops of WE/AgNP were added into the S₁ and S₂ wells producing duplicates of the sample. The samples were prepared by adding 1 mL of WE and AgNP to individually labelled watch glasses and this was allowed to dry in a hot air oven until residues were formed. This was then dissolved in 200µl of d.H₂O and was then added into the wells. Saline (two drops) was used as the negative control and Gentamycin was the positive control. This was then incubated at 37 °C for 24 hours and the zone of inhibition (ZOI) was measured.¹⁶

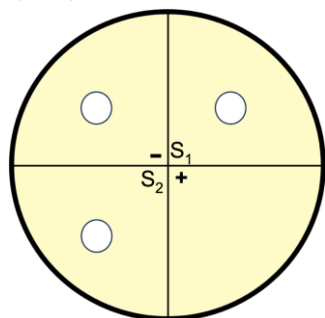


Figure 03: A labelled petri dish with wells only on -, S₁ and S₂

2.14 Statistical Analysis. The results obtained from each of these tests were then tabulated in Microsoft Excel Version 16.75.2 and were subjected to statistical analysis using SPSS. Comparison between species were performed via the one-way Anova test for TFC, TPC, TAC and antibacterial activity. Pearson's correlation was done to observe the correlation between TFC, TPC and TAC.

3. Results

3.1 Qualitative Analysis of Phytochemicals present in the WE

Table 02: Qualitative studies of Phytochemicals present in WE (✓ indicates present and X indicates not present)

Phytochemicals	Red	Durian	MG	Mandarin	Nirosha
Saponins	✓	✓	✓	✓	✓
Glycoside	✓	✓	✓	✓	✓
Alkaloid	✓	✓	✓	✓	✓
Reducing Sugar	✓	✓	✓	✓	✓
Phenols	✓	✓	✓	✓	✓
Flavonoid	✓	✓	✓	✓	✓
Tanins	✓	✓	✓	✓	✓
Carbohydrate	✓	✓	✓	✓	✓
Amino acids	X	X	X	X	X
Anthocyanin	X	X	X	X	X

All the WE showed a positive result for the phytochemicals except for amino acids and anthocyanins.

3.2 Synthesis of AgNP using Jackfruit WE

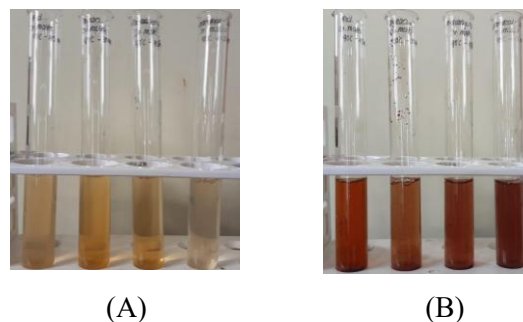


Figure 04: Synthesis of AgNP before (A) and after (B) incubation

Table 03: Optimization of AgNP (✓ indicates synthesized and X indicates not synthesized)

Samples	Incubation at 90 °C				Incubation at 60 °C			
	Time (mins)				Time (mins)			
	60	45	30	15	60	45	30	15

Red	X	✓	X	X	X	X	X	X
Durian	X	X	✓	X	X	X	X	X
MG	X	✓	X	X	X	X	X	X
Mandoor	X	✓	✓	X	X	X	X	X
Nirosha	X	X	X	X	X	X	✓	X

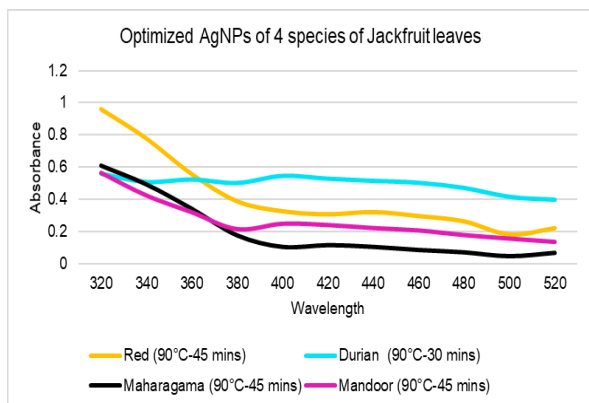


Figure 05: Absorbances of optimized AgNPs of 4 different species of Jackfruit leaves at 90 °C - 45 minutes and 90 °C - 30 minutes.

Red, MG and Mandoor showed the presence of AgNP at 90°C- 45 minutes and Durian and Mandoor showed AgNP presence at 90°C- 30 minutes and AgNP was detected in Nirosha at 60 °C- 30 minutes. A colour change to dark brown was first observed (Figure 04) and the variant 'Durian' had the highest absorbance (Figure 05).

3.3 Bandgap energy of AgNP

Table 04: The band gap energy of AgNP.

Sample	Bandgap energy (eV)	Classifications
Red AgNP	2.82	Semi-conductors
Durian AgNP	3.10	Semi-conductors
MG AgNP	2.95	Semi-conductors
Mandoor AgNP	3.10	Semi-conductors

3.4 SEM Analysis

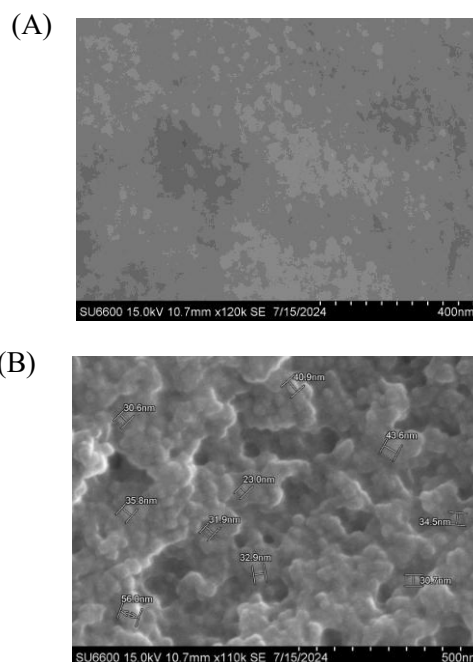


Figure 06: SEM analysis of Red AgNP at 15.0 kV 10.7 mm x 120 k, 400 nm (A) 15.0 kV 10.7 mm x 110 k, 500 nm with diameters (B)

SEM analysis showed spherical shapes of Red AgNP with diameters in the range 20-60 nm.

3.5 Quantitative Analysis of TFC, TPC and TAC of WE and AgNP

3.5.1 TFC

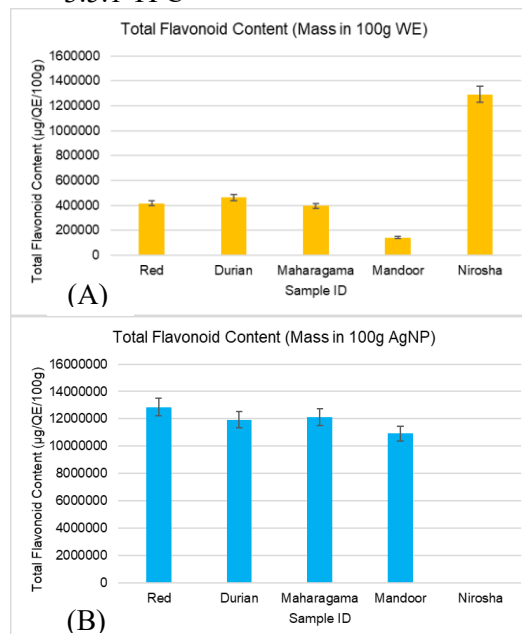


Figure 07: Average TFC of (A) WE and (B) AgNP measured in triplicates

3.5.2 TPC

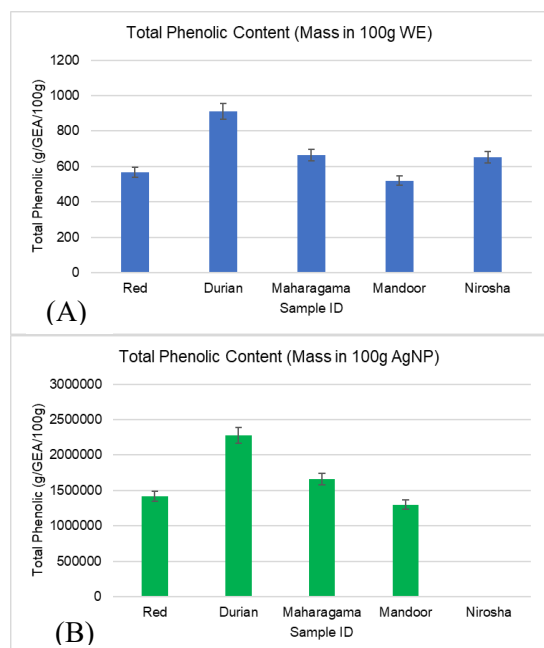


Figure 08: Average TPC of (A) WE and (B) AgNP measured in triplicates

3.5.3 TAC

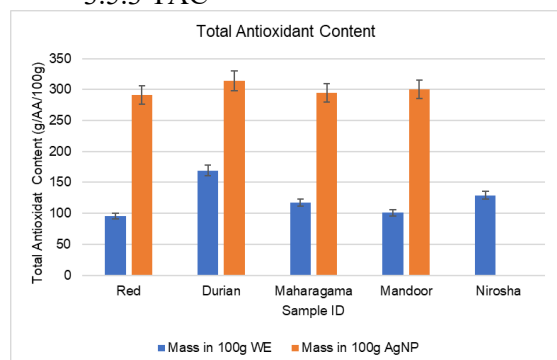


Figure 09: Average TAC of WE and AgNP measured in triplicates

The TFC, TPC and TAC of AgNP were higher than WE and there was a significant difference ($p < 0.05$) between the AgNP and WE.

3.6 Antioxidant Scavenging Activity of WE and AgNP via DPPH assay.

Table 05: IC₅₀ values of WE and AgNP

Sample ID	WE	AgNP
Red	0.36	0.39
Durian	2.43	0.04
MG	0.081	0.39
Mandoor	0.30	0.19
Nirosha	0.13	-

The IC₅₀ of Durian and Mandoor WE were higher compared to their AgNP.

3.7 Cytotoxicity studies of AgNP on Brine shrimps

Table 06: Viability of Brine shrimps in 800 ppm AgNP

Sample	Well 01	Well 02	Well 03	Viability	Results
Red	02/02	02/02	02/02	100%	
Durian	02/02	02/02	02/02	100%	
MG	02/02	02/02	02/02	100%	
Mandoor	02/02	02/02	02/02	100%	
Control	02/02	02/02	02/02	100%	

Table 07: Viability of Brine shrimps in 240 ppm AgNP

Sample	Well 01	Well 02	Well 03	Viability	Results
Red	02/02	02/02	02/02	100%	
Durian	02/02	02/02	02/02	100%	
MG	02/02	02/02	02/02	100%	
Mandoor	02/02	02/02	02/02	100%	
Control	02/02	02/02	02/02	100%	

The results showed that the brine shrimps had a 100% viability in the presence of both 240 ppm and 800 ppm AgNP.

3.8 Degradation PNP using AgNP as a catalyst.

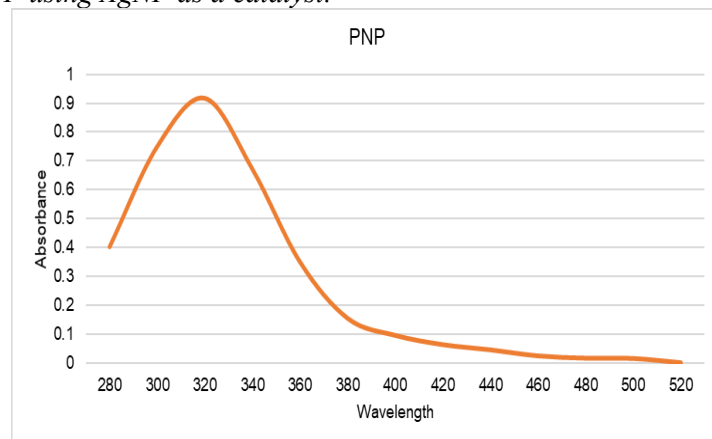


Figure 10: Absorbance of PNP

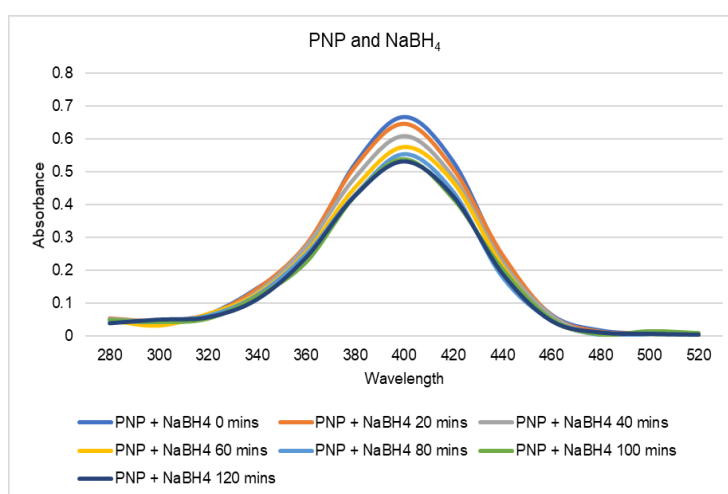


Figure 11: Absorbance during PNP degradation by NaBH₄ over 2 hours (without AgNP)

Degradation was not observed by the addition of NaBH₄ to PNP.

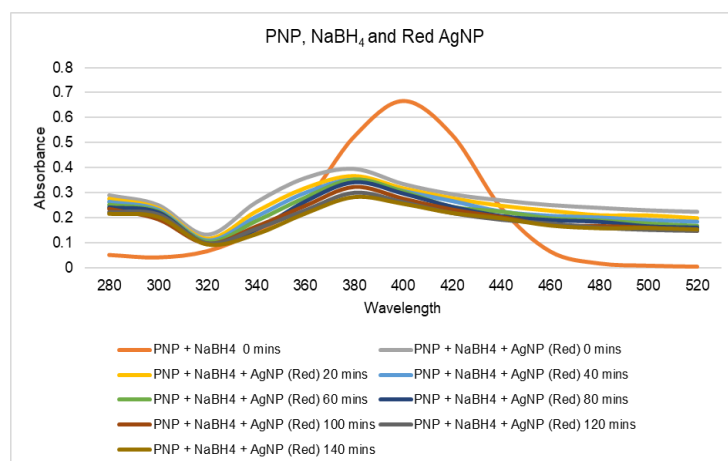
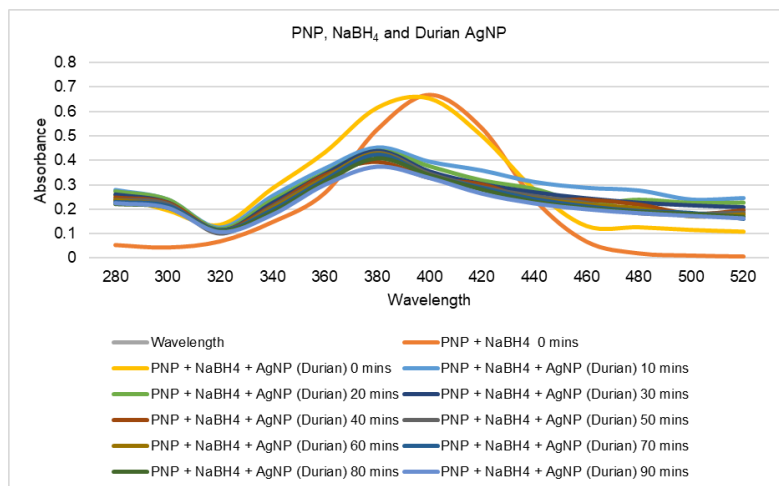
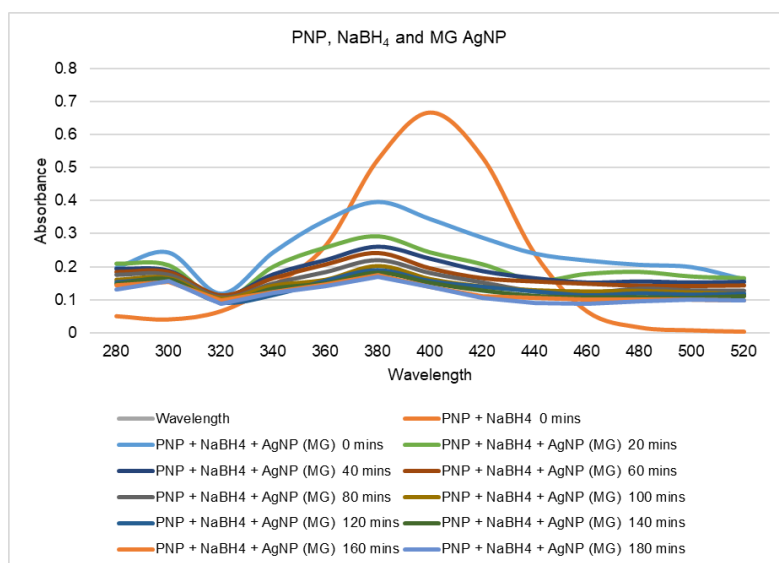
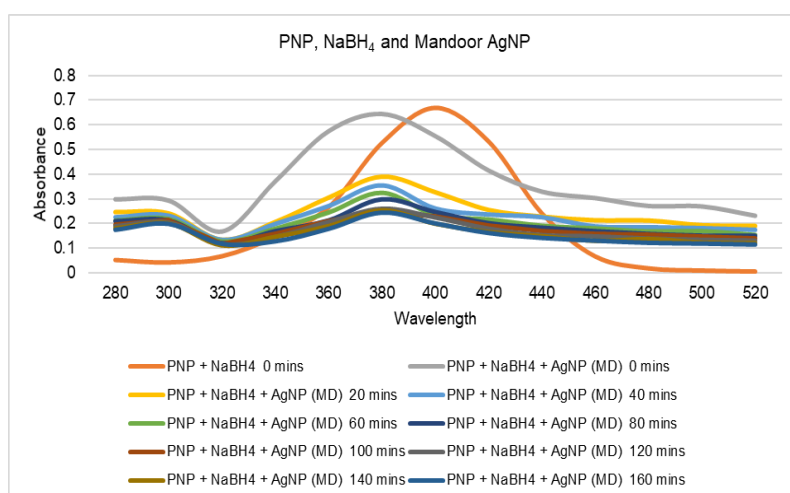


Figure 12: Absorbance of PNP and NaBH₄ in the presence of Red_AgNP

Figure 13: Absorbance of PNP, NaBH₄ in the presence of Durian_AgNPFigure 14: Absorbance of PNP, NaBH₄ in the presence of MG_AgNPFigure 15: Absorbance of PNP, NaBH₄ in the presence of Mandoor_AgNP

PNP degradation was observed with all the AgNP.

3.9 Photocatalytic degradation of MB using AgNP

3.8.1 Degradation of MB under sunlight using AgNP

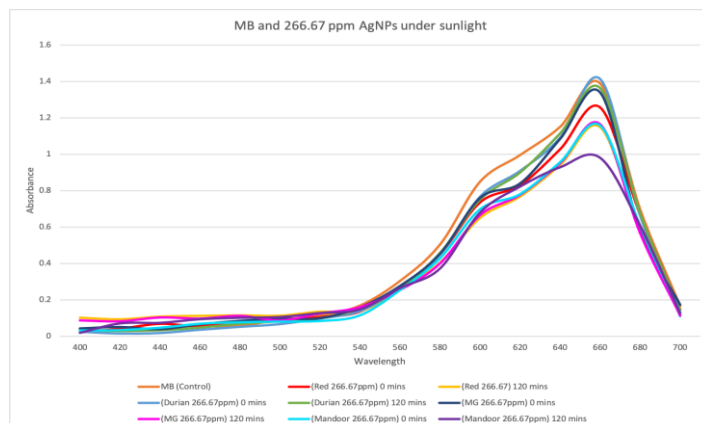


Figure 16: Absorbance of MB and all four 266.67 ppm AgNPs at 0 and 120 minutes

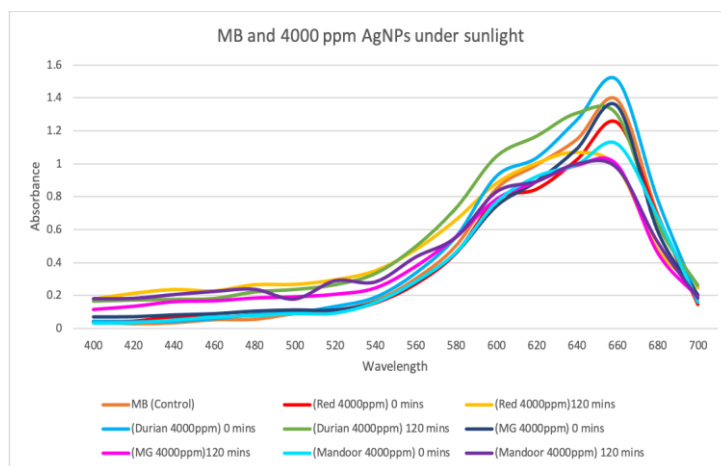


Figure 17: Absorbance of MB and all four 4000 ppm AgNPs at 0 and 120 minutes

MB did not show any degradation with AgNP, under sunlight.

3.8.2 Degradation of MB under sunlight using AgNP and NaBH₄

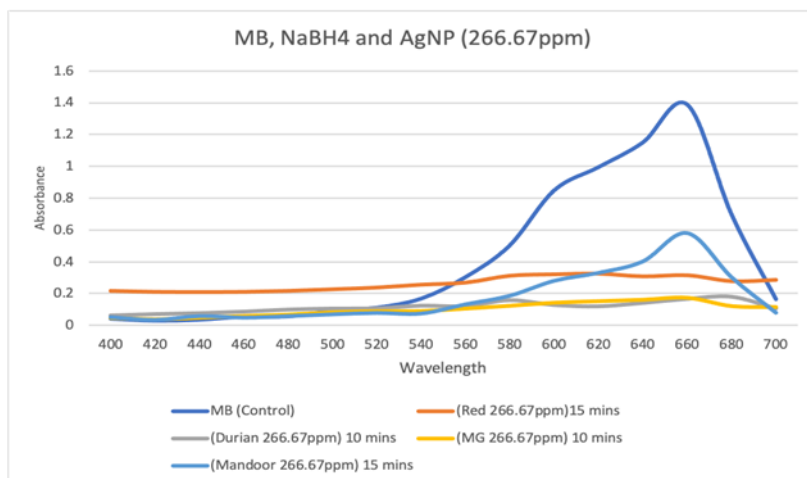


Figure 18: Absorbance of MB, NaBH₄ and all four 266.67 ppm AgNP

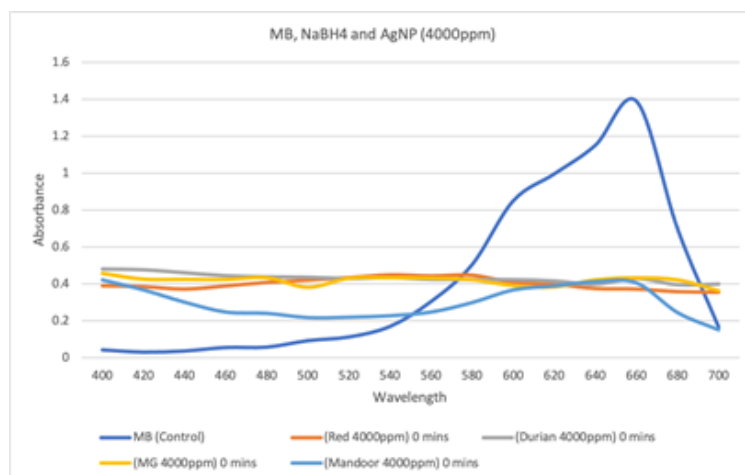


Figure 19: Absorbance of MB, NaBH₄ and all four 4000 ppm AgNP

An instant degradation was observed with 4000 ppm AgNP and NaBH₄ compared to 266.67 ppm and NaBH₄, which took 10-15 mins.

3.10 Melamine adulteration in milk

3.9.1 Detection of melamine in water

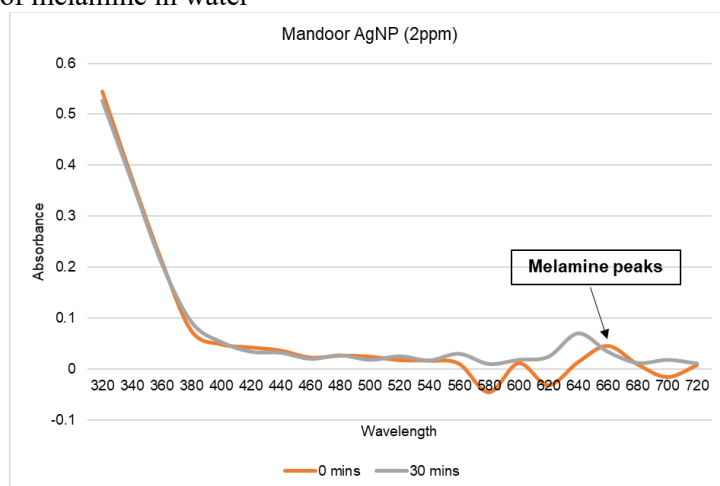


Figure 20: Melamine detection in water (2ppm).

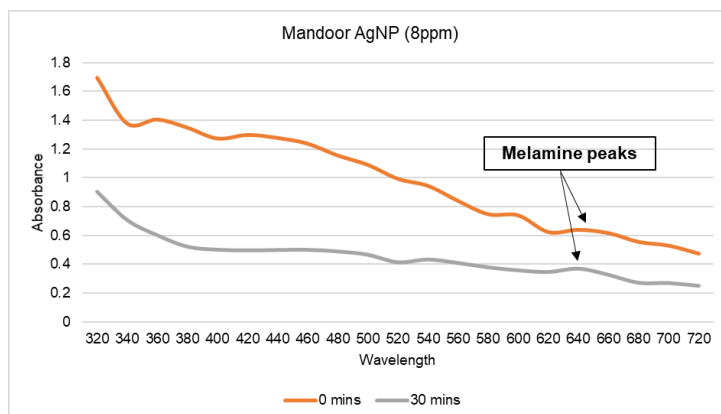


Figure 21: Melamine detection in water (8ppm).

Peaks were observed with 2 ppm and 8 ppm melamine, when spiked in water (Figure 20 and 21).

3.9.2 Melamine adulteration in milk using Mandoor_AgNP

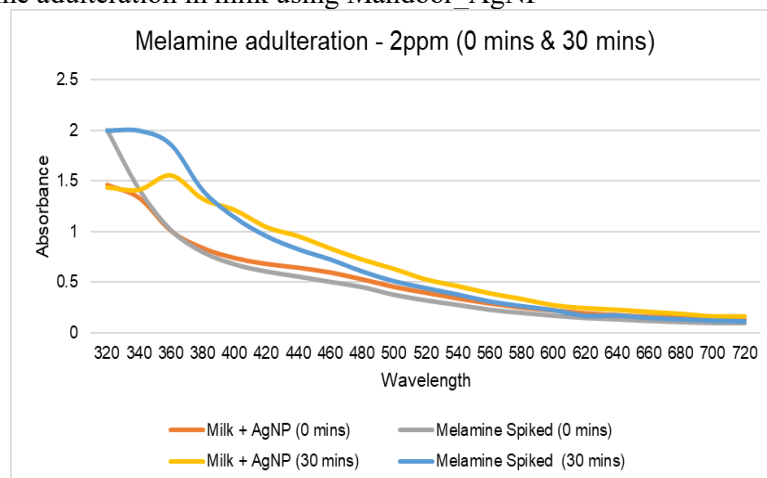


Figure 22: Melamine adulteration in milk (2 ppm)

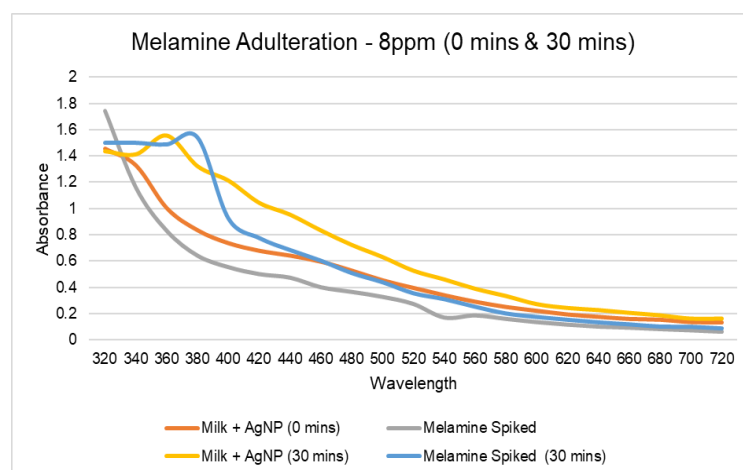


Figure 23: Melamine adulteration in milk (8 ppm).

No peaks were observed in melamine adulteration using milk (Figure 22 and 23).

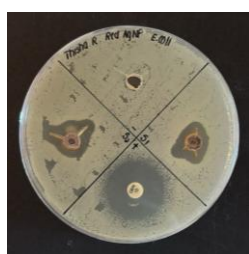
3.11 Antibacterial Activity of WE and AgNP

Table 08: Antibacterial activity of WE and AgNP using *E. coli*

Sample ID	S ₁ (cm)	S ₂ (cm)	Average (cm)	(+) (cm)
Red_WE	-	-	-	2.2
Durian_WE	-	-	-	2.2
MG_WE	-	-	-	2.2
Mandoor_WE	-	-	-	2.4
Nirosha_WE	-	-	-	2.4
Red_AgNP	1.2	1.5	1.35	2.2
Durian_AgNP	1.3	1.3	1.3	2.2
MG_AgNP	1.4	1.3	1.35	2.3
Mandoor_AgNP	1.3	1.2	1.25	2.2

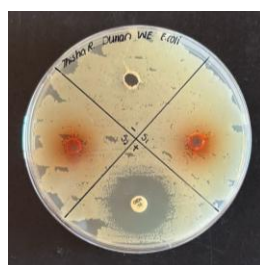


(A)

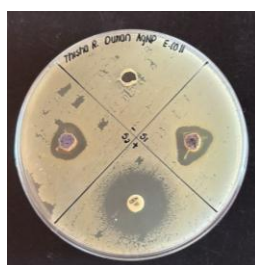


(B)

Figure 24: Antibacterial activity of Red WE (A) and AgNP (B) using *E. coli*



(A)



(B)

Figure 25: Antibacterial activity of Durian WE (A) and AgNP (B) using *E. coli*



(A)



(B)

Figure 26: Antibacterial activity of MG WE (A) and AgNP (B) using *E. coli*



(A)



(B)

Figure 27: Antibacterial activity of Mandoor WE (A) and AgNP (B) using *E. coli*

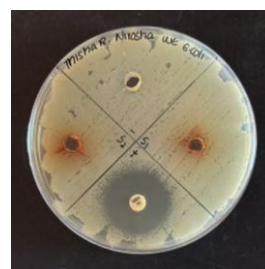
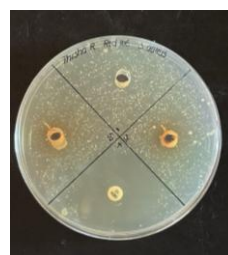


Figure 28: Antibacterial activity of Nirosha WE using *E. coli*

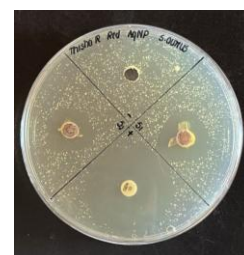
Antibacterial activity was observed in all the AgNP whereas no activity was seen in WE with *E. coli* (Figure 24 - 28).

Table 09: Antibacterial activity of WE and AgNP using *S. aureus*

Sample ID	S ₁ /(cm)	S ₂ /(cm)	Average /(cm)	(+) /(cm)
Red WE	-	-	-	3.5
Durian WE	1.5	1.2	1.35	3.5
MG WE	1.1	1.1	1.1	3.5
Mandoor WE	-	-	-	3.4
Nirosha WE	1.2	1.1	1.45	3.4
Red AgNP	1.4	1.5	1.5	3.3
Durian AgNP	1.5	1.5	1.55	3.4
MG AgNP	1.5	1.6	1.6	3.4
Mandoor_AgNP	1.6	1.6	1.45	3.4



(A)



(B)

Figure 29: Antibacterial activity of Red WE (A) and AgNP (B) using *S. aureus*

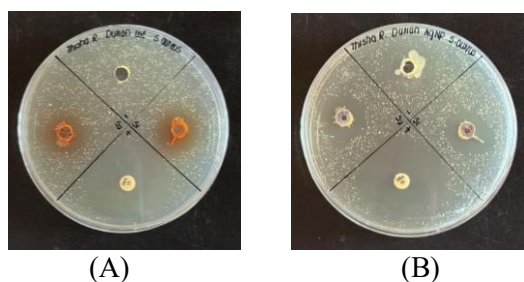


Figure 30 : Antibacterial activity of Durian WE (A) and AgNP (B) using *S. aureus*

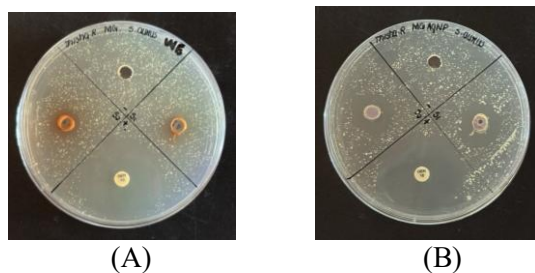


Figure 31 : Antibacterial activity of MG WE (A) and AgNP (B) using *S. aureus*

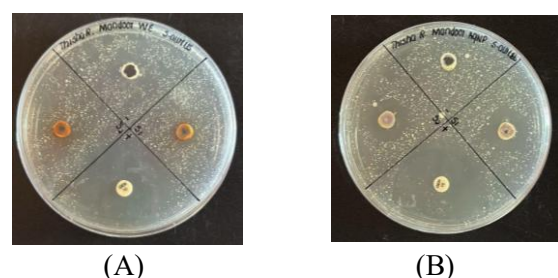


Figure 32: Antibacterial activity of Mandoor WE (A) and AgNP (B) using *S. aureus*



Figure 33: Antibacterial activity of Nirosha WE using *S. aureus*

Antibacterial activities were observed only with Durian, MG and Nirosha WE and all the AgNP showed a ZOI with *S. aureus* (Figure 29-33).

The Anova table showed a p value less than 0.05 ($p = 0.00185$) indicating a significant

difference between the ZOI of *E. coli* and *S. aureus*.

4. Discussion

Jackfruit leaves are usually wasted despite them having many medicinal properties. In addition, research on jackfruit and its parts are limited, altogether, leading us to conducting this research. Since, this research followed the green approach, water was used as the extraction solvent as it is environmentally friendly. Phytochemical analysis showed the presence of saponins, glycosides, alkaloids, reducing sugar, phenols, flavonoids, tannins and carbohydrates in WE.¹⁹ However, negative results were obtained for both amino acids and anthocyanins.

Ag^+ is reduced to Ag by the phytochemicals present in the plants as in Figure 34. Phytochemicals act as stabilizing, reducing and capping agents, resulting in AgNP formation.⁵² Nanoparticle synthesis is affected by the incubation time, temperature, components/concentrations of WE, pH and metal ion concentrations.¹⁸

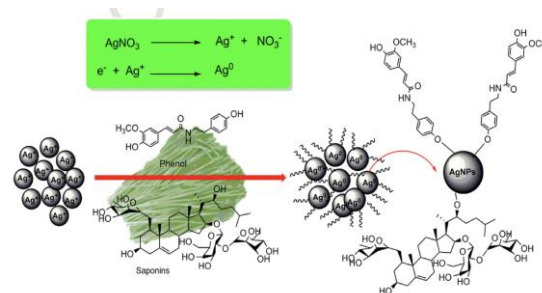


Figure 34: Green synthesis of AgNP.²⁸

The first observation was a colour change from pale yellow to dark brown (Figure 04) due to the excitation of the Surface Plasmon Resonance (SPR). The oscillations of the conductive electrons on the AgNP surface due to excitation by light is known as the SPR.²⁸ Red, MG and Mandoor showed AgNP at 90 °C - 45 minutes whereas at 90 °C - 30 minutes, AgNP was detected in Durian and Mandoor and at 60 °C - 30 minutes for Nirosha. These temperatures were also observed with Anu and her team.⁴ The detection of AgNP in the range 400-500 nm is also due to the SPR.⁵

Semi-conductors have a bandgap energy $< 3\text{eV}$ and insulators have a bandgap energy $> 4\text{eV}$. Since some AgNP had a bandgap energy $> 3\text{eV}$

but <4eV (Table 04), they were also classified as semi-conductors.

The shape and size of Red_AgNP was determined using SEM.⁶ SEM analysis showed spherical AgNP of sizes in between 20-60nm (Figure 06), similar findings were also shown by Manjare.⁴¹ However, AgNP clustering was observed²⁷ and this could be due to the increased Ag⁺ concentration or increased pH of the extracts.⁹

The principles of TFC, shown in Figure 35, involves AlCl₃ forming a stable acid complex with the ketone groups along with the orthodihydroxyl group of the flavonoids, giving a yellow colour.³⁸ The TFC of AgNP were higher than their WE. TFC was high in Nirosha_WE and Red_AgNP (Figure 07). A p value of 2.14x10⁻⁸, shows a significant difference between AgNP and WE.

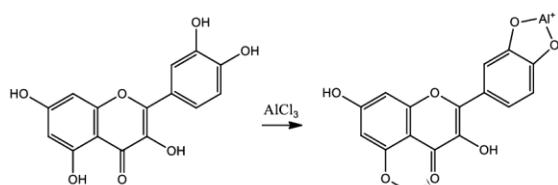


Figure 35: Principles of quantitative TFC.³⁷

In TPC, the oxidation of the phenol group by the FCR enables the reduction of the phosphomolybdate-phosphotungstate in the FCR into molybdenum-tungsten complex (Figure 36), giving rise to a blue complex. Na₂CO₃ provides an alkaline atmosphere which facilitates the dissociation of protons from the phenolic compound.⁴⁹

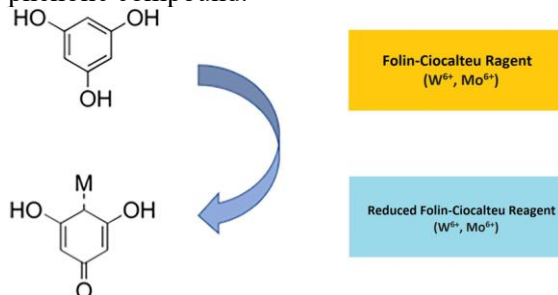


Figure 36: Principles of quantitative TPC.⁶²

The TPC of AgNP was higher than the WE. Durian_WE and AgNP showed the highest TPC value (Figure 08). A p value of 5.37x10⁻⁵ (p < 0.05) suggests a significant difference between the TPC of the WE and AgNP.

TAC assay involves the reduction of molybdenum (VI) into molybdenum (V) in the presence of an antioxidant, giving a greenish-blue colour (Figure 37). The TAC of AgNP was higher than the WE and Durian_WE and AgNP had the highest TAC value (Figure 09). A p value of 8.67x10⁻⁶ (p < 0.05) shows a significant difference between the WE and AgNP. However, studies were not conducted on Jackfruits to support this.

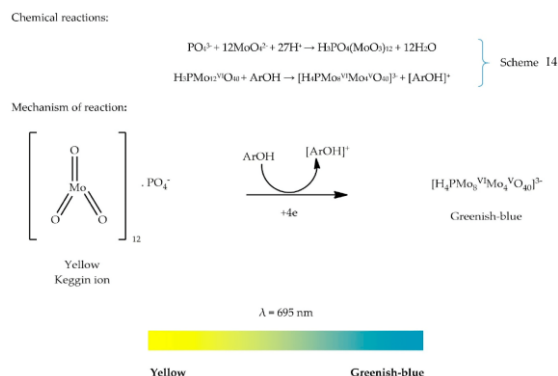


Figure 37: Principles of Quantitative TAC.⁵⁹

The TFC, TPC and TAC of the AgNP were higher than their respective WE. However, the increase in TFC and TPC in WE compared to AgNP¹⁷ could be due to different locations, variants and the involvement of the phytochemicals during AgNP synthesis.⁶⁷

A strong correlation was observed among TFC, TPC and TAC in the Pearson correlation analysis (Figure 38). The TFC-TAC was higher compared to the others, indicating that flavonoids were the predominant phenolic compounds in jackfruit leaves that attributed to their antioxidant activities.⁷⁸

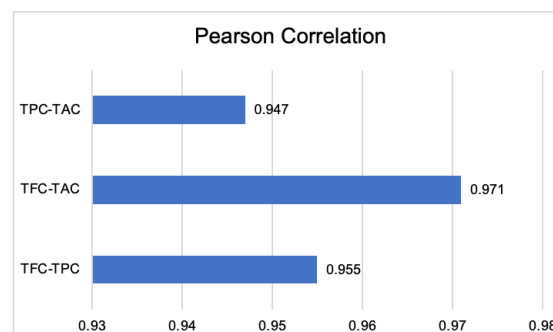


Figure 38: Pearson correlation between TFC, TPC and TAC

DPPH is a stable free radical that contains free electrons in its nitrogen atom which can be reduced by the H atom of the antioxidant.

DPPH has a deep purple colour which changes to pale yellow colour when it is reduced. There is a strong absorbance at 517 nm due to the presence of an odd electron. The AgNP's antioxidant activity, in Figure 39, is due to the bioactive molecules and secondary metabolites on the AgNP surface.³⁰

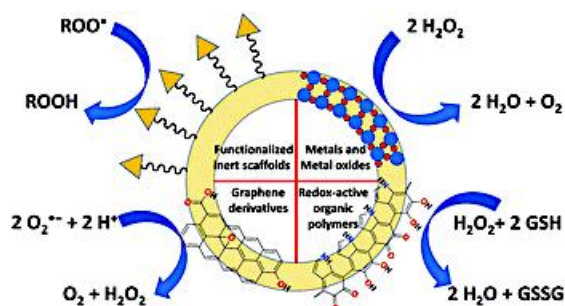


Figure 39: Antioxidant activity of Nanoparticles.⁶⁹

The IC_{50} is the concentration of an antioxidant-containing substance required to scavenge 50% of the initial DPPH radicals.⁴⁸ A high antioxidant activity is indicated by a low IC_{50} value. The results showed that Durian and Mandoor WE along with Red and MG AgNP had higher antioxidant activities (low IC_{50}) than their respective AgNP/WE.²⁶ Antioxidant activity of WE could be due to their increased phenolic and flavonoid content.¹⁷

AgNP's cytotoxic effect involves the interaction between the chitin of the brine shrimp and the Ag^+ ions, leading to the deformation of the chitin structure and eventually death.⁵¹ AgNP can also enter the cell through diffusion or endocytosis. AgNP or Ag^+ generates ROS and elevated ROS levels produces oxidative stresses which eventually results in damage to the DNA and proteins in the cell leading to cell apoptosis,³ as shown in Figure 40.

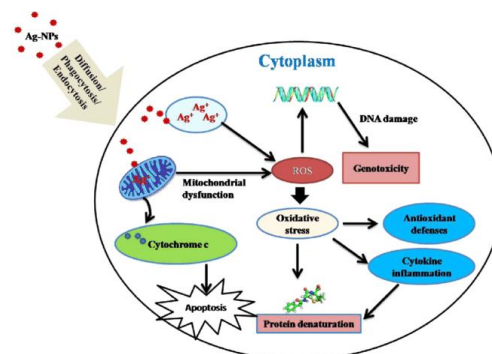


Figure 40: Cytotoxicity of AgNP.³

However, the brine shrimps had a 100% viability with 240 ppm and 800 ppm AgNP, due to the production of AgNP via green synthesis. Phytochemicals involved in nanoparticle formation are usually compatible with the biological systems, resulting in a decreased cytotoxicity.⁷⁰

PNP has 2 different absorbances based on its pH, 317 and 400 nm. In acidic conditions, a peak at 317nm is observed and upon the addition of $NaBH_4$, the peak shifts to the right and forms at 400nm (Figure 10).⁷³ PNP degradation to p-aminophenolate (PAP) by $NaBH_4$ is kinetically too slow due to the presence of a potential difference and a kinetic barrier between the donor (borohydride) and the acceptor (p-nitrophenolate ions), therefore, a slow degradation was observed with PNP and $NaBH_4$ (Figure 11).

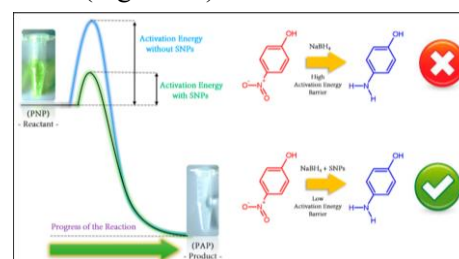


Figure 41: Catalytic degradation of PNP by AgNP.⁶³

With AgNP, the addition of $NaBH_4$, forms hydrogen gas, which is adsorbed onto the AgNP. Thereafter, the adsorption of p-nitrophenolate ions onto the AgNP allows the reduction process, eventually causing the desorption of PAP from the AgNP. Hence, acting as a catalyst by facilitating the transfer of electrons from the donor to the acceptor and thus overcoming the kinetic barrier,⁶³ demonstrated in Figure 41. A colour change

from yellow to colourless also shows the degradation of PNP to PAP.⁵³

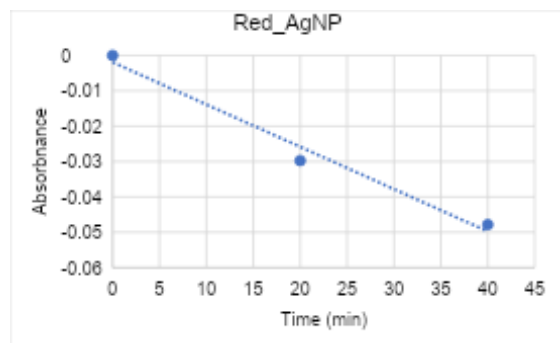


Figure 42: The rate of reaction for Red_AgNP

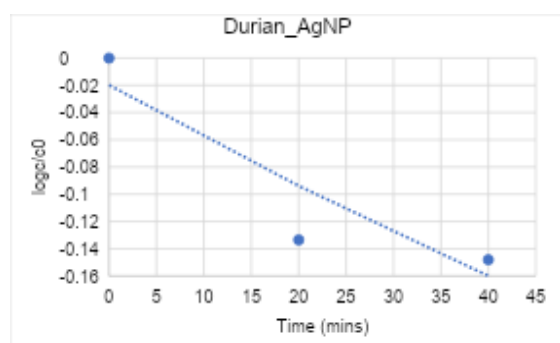


Figure 43: The rate of reaction for Durian_AgNP

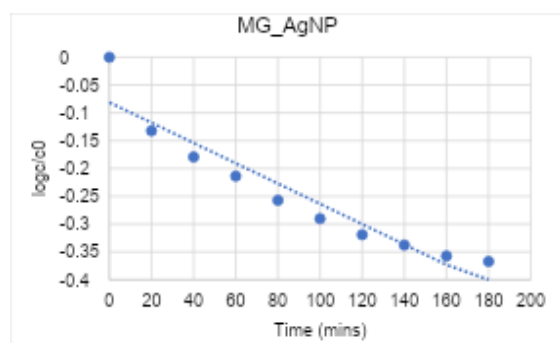


Figure 44: The rate of reaction for MG_AgNP

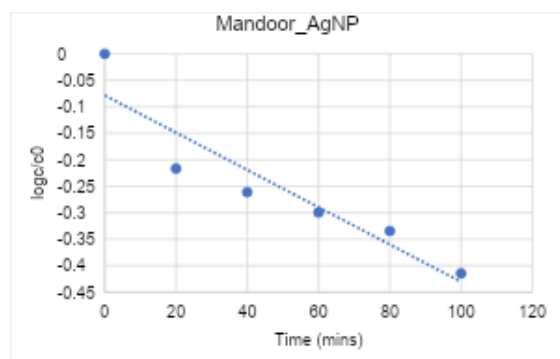


Figure 45: The rate of reaction for Mandoor_AgNP

Table 10: Rate constants of AgNP

Sample	Rate constant K
Red AgNP	0.0012
Durian AgNP	0.0037
MG AgNP	0.0018
Mandoor AgNP	0.0035

The reaction rate increased in the order Red < MG < Mandoor < Durian AgNP, shown in Figures 42-45 and table 10.

MB degradation by AgNP involves the excitation of the electrons in the VB into the CB upon irradiation. This generates an electron-hole which results in the production of hydroxyl radicals, which acts as an oxidizing agent, leading to the degradation of MB,⁴² shown in Figure 46. In the presence of NaBH₄, adsorption of the BH₄⁻ onto the AgNP facilitates the transfer of electrons to MB eventually leading to a faster degradation,²² explaining why there was no visible degradation of MB under sunlight, in the absence of NaBH₄.

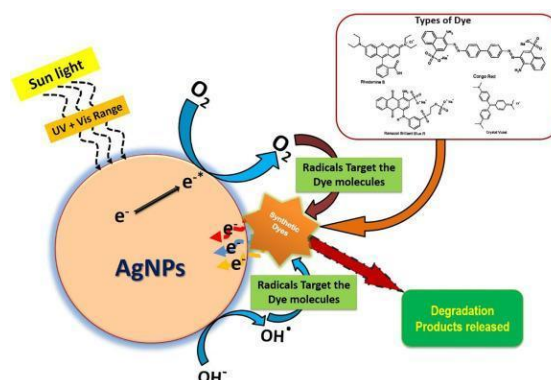


Figure 46: Photocatalytic degradation of MB using AgNP.⁴²

With high concentrations of AgNP, there is an increased dispersion and an increased availability of active sites, explaining why an instant degradation of MB was observed with 4000 ppm AgNP and NaBH₄, whereas 10-15 minutes was needed for the complete degradation of MB using 266.67 ppm AgNP. The increase in absorbance observed with 4000 ppm AgNP and NaBH₄ after 0 minutes could be due to the agglomeration of excess AgNP.⁶⁸

Since melamine has a high nitrogen content, it is used in milk adulteration.⁵⁶ AgNP plays a role in melamine detection via the electrostatic interaction between the negatively charged nanoparticle surface and the positively charged

amino group of melamine. The aggregation of the AgNP results in a colour change from yellow to red,⁵⁴ shown in Figure 47. A peak in the range 600 nm corresponds to the conversion of the dispersed AgNP into its aggregated form.⁶⁴

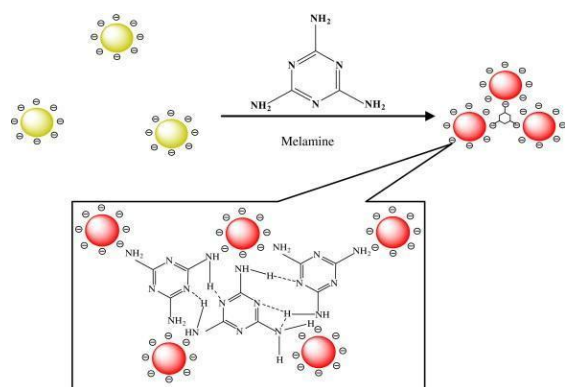


Figure 47: The MOA of Melamine detection by AgNP.⁵⁰

Even though Mandoor_AgNP detected melamine (2ppm and 8ppm) in water, in milk, no peaks were observed for both AgNP and melamine, showing the absence of melamine in milk. The absence of AgNP peaks (Figure 22, 23), could be due to the interaction between existing whey proteins and AgNP, which inhibits the binding of melamine to the AgNP. However, this point was not proven with AgNP but this phenomenon was observed with gold nanoparticles,⁴³ assuming this could be the same with AgNP.

The AgNP exhibits its antibacterial activity by accumulating in the pits formed on the cell wall when they attach themselves, leading to the disruption of the cell wall and membrane permeability. The main MOA involves the release of Ag^+ from AgNP, which attaches to the bacterial cell wall and membrane via electrostatic interactions between the sulfur proteins, increasing the permeability of the cell membrane. Upon the penetration of the cell membrane, the Ag^+ deactivates the respiratory enzymes leading to the production of reactive oxidative species (ROS) which causes damage to the DNA. Since the DNA mainly consists of phosphate and sulphur, the Ag^+ interacts with the DNA affecting DNA replication. Furthermore, protein synthesis is also inhibited

due to denaturation of the ribosome components,¹ shown in Figure 48.

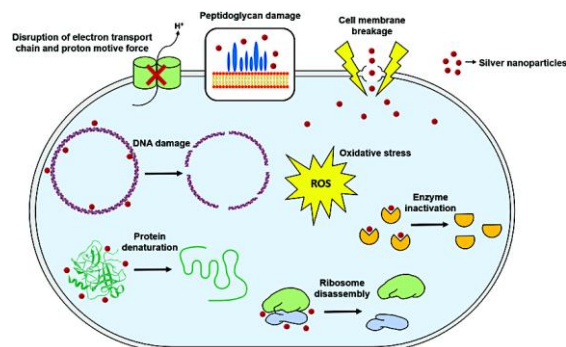


Figure 48: Antibacterial activity of AgNP.⁵⁸

A ZOI was observed with all the AgNP in both *E. coli* and *S. aureus* but no ZOI was seen with WE in *E. coli*. However, Durian, MG and Nirosha WE showed a ZOI with *S. aureus*. This is due to the presence of phytochemicals, which gives WE their antibacterial properties, supported by the studies from Dhierllate.²¹ The AgNP was more potent against *S. aureus* compared to *E. coli*, similar results were observed by Manjare.⁴¹ The reason behind *S. aureus* being more sensitive to AgNP could be due to the lack of an outer film surrounding the peptidoglycan layers of the cell wall, allowing the straightforward interaction of AgNP and the bacterial outer membrane.⁷⁴ A p value of 0.002 shows a significant difference between the ZOI of *S. aureus* and *E. coli*.

5. Conclusion

In conclusion, AgNP was synthesized from 5 different variants of Jackfruit leaves. Optimization of AgNP occurred at 90 °C -30 and 45 minutes and at 60 °C - 30 minutes. All the AgNP were classified as semi-conductors. SEM analysis showed spherical AgNP of diameters between 20-60 nm. TFC, TPC and TAC were high in AgNP compared to their WE. The IC_{50} of Durian and Mandoor WE were found to be higher than their AgNP. Cytotoxicity study using *Artemia salina* showed 100% viability. Faster degradation of PNP was observed in Durian AgNP. The photocatalytic degradation of MB was also rapid with all AgNP and NaBH_4 . Mandoor_AgNP detected melamine in water but not in milk. All the AgNP showed antibacterial activity against *S. aureus* and *E. coli* and was more potent against *S. aureus*.

Therefore, AgNP synthesized from Jackfruit leaves can be used in many industries.

References

1. S. Ahmad, S. Das, A. Khatoon, M. Ansari, , M. Afzal, , S. Hasnain and A. Nayak. *Materials Science for Energy Technique*. 2020;**3**(20);756-769.
2. R. Ahmed and D. Mustafa. *International Nano Letters*. 2019;**10**;1- 14.
3. M. Akter, M. Rahman, T. Sikder, A. Ullah, K. Hossain, S. Banik, T. Hosokawa, T. Saito and M. Kurasaki. *Journal of Advanced Research*. 2017;**9**;1-16.
4. V. Anu, R. Methi, C. Mujeeb and M. Vinod. *International Journal of Research in Pharmaceutical and Nano Sciences*. 2015;**4**(1).
5. J. Ashraf, M. Ansari, H. Khan, M. Alzohairy and I. Choi. *Scientific Reports*. 2016;**6**.
6. M. Asif, R. Yasmin, R. Asif, A. Ambreen, M. Mustafa and S. Umbreen. *Green Dose Response*. 2022;**20**(2).
7. Ö. Aslantürk. Genotoxicity – A Predictable Risk to Our Actual World. 2018.
8. C. Banti and S. Hadikakou. *Bio Protocol*. 2021;**11**(2).
9. S. Bashkova, D. Plata, E. Aguado, J. Carollo. *Preprints. org*. 2024.
10. S. Bayda, M. Adeel, T. Tuccinardi, M. Cordani and F. Rizzolio. *Molecules*. 2019;**25**(1);112.
11. Z. Bedlovičová, I. Strapáč, M. Baláz, A. Salayová. *Molecules*. 2020;**25**(14);3191.
12. K. Bhardwaj, D. Dhanjal, A. Sharma, E. Nepovimova, A. Kalia, S. Thakur, S. Bhardwaj, C. Chopra, R. Singh, R. Verma, D. Kumar, P. Bhardwaj and K. Kuča. *International Journal of Molecular Sciences*. 2020;**21**(9028).
13. V. Bhat, A. Mutha and M. Dsouza. *International Journal of ChemTech Research*. 2017;**10**(9);525.
14. T. Bruna, F. Maldonada-Bravo, P. Jara and N. Caro. *International Journal of Molecular Science*. 2021;**22**(13);7202.
15. A. Burduşel, O. Gherasim, A. Grumezescu, L. Mogoantă, A. Ficai and E. Andronescu. *Nanomaterials*. 2018;**8**(9).
16. S. Charannya, D. Duraivel, K. Padminee, S. Poorni, C. Nishanthine and M. Srinivasan. *Contemporary Clinical Dentistry*. 2018;**9**(Suppl 2);S204-S209.
17. R. Chavan, M. Bhutkar and S. Bhinge. *Nano Biomedicine and Engineering*. 2023;**15**(3).
18. D. Chugh, V. Viswamalya, B. Das. *Journal of Genetic Engineering and Biotechnology*. 2021;**19**(1).
19. S. Devi, N. Kumar and K. Sabu. *Future Journal of Pharmaceutical Sciences*. 2021;**7**(1);1-7.
20. A. Dhaka, S. Mali, S. Sharma, R. Trivedi. *Results in Chemistry*. 2023;**6**(1);101108.
21. F. Dhierllate, P. Campos, O. Aline. *Food Science and Technology (Campinas)*. 2021;**42**;8-9.
22. A. Fairuzi, N. Bonnia, M. Akhri, M. Abrani and H. Akil. *IOP Conference Series: Earth and Environmental Science*. 2018;**105**(1).
23. H. Fleischer. *World Journal of Chemical Education*. 2019;**7**(2).
24. M. Fouad, L. Shihata, E. Morgan. *Renewable and Sustainable Energy Reviews*. 2017;**80**(1);1499-1511.
25. V. Hajhashemi, G. Vaseghi, M. Pourfarzam and A. Abdollahi. *A Research in Pharmaceutical Sciences*. 2010;**5**(1);1-8.
26. M. Insanu, H. Pramasatya, A. Buddhisuharto, C. Tarigan, A. Zahra, A. Haniffadi, N. Sabila and I. Fidrianny. *Journal of Medical Sciences*. 2022;**10**(A).
27. U. Jagtap and V. Bapat. *Industrial Crops and Products*. 2013;**46**(2013);132-137.
28. F. Jalilian, A. Chahardoli, K. Sadrjavadi, A. Fattahi and Y. Shokoohinia. *Advanced Power Technology*. 2020;**31**(3);1323-1332.
29. C. Kästner and A. Thünemann. *Langmuir*. 2016;**32**(29);7383-7391.
30. A.K. Keshari, R. Srivastava, P. Singh, V. Yadav, and G. Nath. *Journal of Ayurveda and Integrative Medicine*. 2020;**11**(1);37-44.
31. H. Khoo, A. Azlan, S. Tang, S. Lim. *Food & Nutrition Research*. 2017;**61**(1).
32. D. Kumar, P. Kumar, H. Singh, V. Agrawal. *Environmental Science and Pollution Research*. 2020;**27**(11).
33. M. Kumar, N. Supraja and E. David. *Novel Research in Sciences*. 2019;**2**(2).
34. N. Kumar, H. Kumar, B. Mann, R. Seth. *Spectrochimica Acta Part A: Molecular and Biomolecular Spectroscopy*. 2016;**156**;89-97.
35. D. Latha, C. Arulvasu, P. Prabu, V. Narayanan. *Materials Science & Engineering*. 2017.
36. S. Lee and B. Jun. *Silver Nanoparticles: International Journal of Molecular Sciences*. 2019;**20**(4);865.
37. A. Lu'ma and M. Anggarani. *Prisma Sains Jurnal Pengkajian Ilmu dan Pembelajaran Matematika dan IPA IKIP Mataram*. 2022; **10**(3);658.
38. D. Makuasa and P. Ningsih. *Journal of Applied Science Engineering Technology and Education*. 2020;**2**(1);11-17.
39. UP. Manik, A. Nande, S. Raut, S.J. Dhoble. *Results in Materials*. 2020;**6**;100086.
40. T. Manimekalai and P. Chitra. *Journal of University of Shanghai for Science and Technology*. 2021;**23**(6);1554-1568.
41. S. Manjare, P. Paranjape, V. Gurav, P. Shinde, R. Chavan and S. Thopate. *Bioinspired, Biomimetic and Nanobiomaterials*. 2019;**9**(3);1-5.
42. S. Marimuthu, A. Antonisamy, S. Malayandi, K. Rajendran, P. Tsai, A. Pugazhendhi and V. Ponnusamy. *Journal of Photochemistry and Photobiology B: Biology*. 2020;**205**(12);111823.
43. S. Mi, Y. Du, F. Gao, S. Yuan, H. Yu, Y. Guo, Y. Cheng, G. Li and W. Yao. *Food Chemistry*. 2024;**459**;140416.
44. M. Moond, S. Singh, S. Sangwan, S. Rani, A. Beniwal, J. Rani, A. Kumari, I. Rani and P. Devi. *International Journal of Molecular Science*. 2023;**24**(4);3480.
45. S. Murthy. *Nanoparticles in modern medicine: International Journal of Nanomedicine*. 2007;**2**(2);129-141.
46. A. Nyabadza, E. McCarthy, M. Makhesana, S. Heidarinassab, A. Plouze, M. Vazquez and D. Brabazon. *Advances in Colloid and Interface Science*. 2023;**321**(4);103010.
47. RA. Ojwang, EK. Muge, B. Mbatia, B. Mwanza and D. Ogoyi. *Journal of Advances in Biology & Biotechnology*. 2017;**16**(1);1-13.

48. JO. Olugbami, MA. Gbadegesin and OA. Odunola. *Afr J Med Med Sci*. 2014;**43**(Suppl 1);101-109.
49. M. Pérez, I. López and R. Raventós. *Journal of Agriculture and Food Chemistry*. 2023;**71**(46).
50. H. Ping, M. Zhang, H. Li, S. Li, Q. Chen, C. Sun and T. Zhang. *Food Control*. 2012;**23**(1);191-197.
51. S. Pinheiro, A. Lima, T. Miguel, A. Filho, O. Ferreira, M. Pontes, R. Grillo and E. Miguel. *Chemosphere*. 2024;**347**;140673.
52. M. Pradeep, D. Kruszka, P. Kachlicki, D. Mondal and G. Franklin. *ACS Sustainable Chemistry Engineering*. 2022;**10**(1);562-571.
53. P. Rajegaonkar, B. Deshpande, M. More, S. Waghmare, V. Sangwe, A. Inamdar, M. Shirsat and N. Adhapure. *Materials Science and Engineering: C*. 2018;**93**;623-629.
54. K. Ramalingam, T. Devasena, B. Senthil, R. Kalpana and R. Jayavel. *The Institution of Engineering and Technology*. 2017;**11**(2).
55. R. Ranasinghe, S. Maduwanthi and R Marapana. *International Journal of Food Science*. 2019;**2019**(6);1-12.
56. M. Ritota and P. Manzi. *Melamine Food Analytical Methods*. 2017;**11**(1);128-147.
57. K. Rovina and S. Siddiquee. *Journal of Food Composition and Analysis*. 2015;**43**;25-38.
58. A. Roy, O. Bulut, S. Some, A. Mandal and M. Yilmaz. *Royal Society of Chemistry*. 2019;**9**(5);2673-2702.
59. NB. Sadeer, D. Montesano, S. Albrizio, G. Zengin and M.F. Mahomoodally. *Antioxidants*. 2020;**9**(8);709.
60. S. Sana, R. Haldhar, J. Parameswaranpillai, M. Chavali, and S. Kim. *Cleaner Materials*. 2022;**6**(6);100161.
61. S. Sharmin, B. Islam, B. Saha, F. Ahmed, B. Maitra, Z. Rasel, , N. Quaisaar and A. Rabbi. *Heliyon*. 2023;**9**(10).
62. L. Shi, W. Zhao, Z. Yang, V. Subbiah and H.A. Suleria. *Environmental Science and Pollution Research*. 2022;**29**(54).
63. G. Shimoga, R. Palem, S. Lee and S. Kim. *Metals*. 2020;**10**(12).
64. S. Siddiquee, S. Saallah, N. Bohari, G. Ringgit, J. Roslan, L. Naher and N. Nudin. *Nanomaterials*. 2021;**11**(5);1142.
65. S. Tang and J. Zheng. *Antibacterial Advanced Healthcare Material*. 2018;**7**(13);1701503.
66. N. Thapa, P. Thapa, J. Bhandari, P. Niraula, N. Shrestha and B. Shrestha. *Nepal Journal of Biochemistry*. 2016;**4**(1);47-53.
67. S. Thirumal. *International Journal of Botany Studies*. 2021;**6**(3);476-480.
68. Q. Trieu, C. Le, C. Pham and T. Bui. *Journal of Experimental Science*. 2023;**18**(1).
69. L. Valgimigli, A. Baschieri and R. Amorati. *Journal of Materials Chemistry B*. 2018.
70. A. Velidandi, S. Dahariya, N. Pabbathi, D. Kalivarathan and R. Baadhe. *NanoWorld Journal*. 2020;**6**(3);35-60.
71. M. Wang, S. Marepally, P. Vemula and C. Xu. *Nanoscience in Dermatology*. 2016;57-72.
72. A. Wongklom, K. Siriwan and S. Krairam. *Creative Science*. 2023;**15**(1).
73. H. Xia, W. Zhang, Z. Yang, Z. Dai and Y. Yang. *Journal of Analytical Methods in Chemistry*. 2021;**2021**;6682722.
74. Y. Xing, X. Liao, X. Liu, W. Li, R. Huang, J. Tang, Q. Xu, X. Li and J. Yu. *Materials*. 2021;**14**(19);5878.
75. J. Xu, B. Wang, W. Zhang, F. Zhang, Y. Deng, Y. Wang, J. Gao, Y. Tian, R. Peng and Q. Yao. *AMB Express*. 2021;**11**(1);124.
76. L. Xu, Y. Wang, J. Huang, C. Chen, , Z. Wang and H. Xie. *Theranostics*. 2020;**10**(20);8996-9031.
77. X. Zhang, Z. Liu, W. Shen and S. Gurunathan. *International Journal of Molecular Sciences*. 2016;**17**(9);1534.
78. Z. Zhu, B. Zhong, Z. Yang, W. Zhao, L. Shi, A. Aziz, A. Rauf, A. Aljohani, F. Alhumaydhi and H. Suleria. *ACS Omega*. 2022;**7**(17);14630-14642.
79. C. Divan, V. Mohanapriya, M. Jiri and P. Michal. *Polymers*. 2020;**12**(4).

Acknowledgement

Special thanks to BMS for providing a workplace, the required equipment and reagents to work with to carry out the research. Authors would also like to thank SLINTEC, for allowing us to perform SEM analysis.